An Extreme Event in the Eyewall of Hurricane Felix on 2 September 2007

SIM D. ABERSON

NOAA/Atlantic Oceanographic and Meteorological Laboratory/Hurricane Research Division, Miami, Florida

JUN A. ZHANG

University of Miami/Cooperative Institute for Marine and Atmospheric Studies, and NOAA/Atlantic Oceanographic and Meteorological Laboratory/Hurricane Research Division, Miami, Florida

KELLY NUÑEZ OCASIO[a]

University of Puerto Rico at Mayagüez, Mayagüez, Puerto Rico

(Manuscript received 20 September 2016, in final form 6 March 2017)

ABSTRACT

During a routine penetration into Hurricane Felix late on 2 September 2007, NOAA42 encountered extreme turbulence and graupel, flight-level horizontal wind gusts of over 83 m s^{-1}, and vertical wind speeds varying from 10 m s^{-1} downward to 31 m s^{-1} upward and back to nearly 7 m s^{-1} downward within 1 min. This led the plane to rise nearly 300 m and then return to its original level within that time. Though a dropwindsonde was released during this event, the radars and data systems on board the aircraft were rendered inoperable, limiting the amount of data obtained.

The feature observed during the flight is shown to be similar to that encountered during flights into Hurricanes Hugo (1989) and Patricia (2015), and by a dropwindsonde released into a misovortex in Hurricane Isabel (2003). This paper describes a unique dataset of a small-scale feature that appears to be prevalent in very intense tropical cyclones, providing new evidence for eye–eyewall mixing processes that may be related to intensity change.

1. Introduction

During late August 2007, the National Oceanic and Atmospheric Administration (NOAA) planned a series of research aircraft missions into a developing tropical disturbance east of the Lesser Antilles in order to obtain airborne Doppler radar data to test its assimilation into high-resolution numerical models. The two P3 aircraft, based in St. Croix, U.S. Virgin Islands, began twice-daily, staggered, single-plane missions into Tropical Storm Felix on 1 September (Brennan et al. 2009). Three consecutive flights were conducted (Table 1), and, during that time, Felix underwent rapid intensification. The National Hurricane Center (NHC) Special Discussion Number 10 listed a remarkable set of data from the third P3 flight (aircraft NOAA42) that supported category 5 intensity: 1) a peak flight-level wind speed of 152 kt (78.2 m s^{-1}), 2) peak surface wind speeds from the stepped-frequency microwave radiometer (SFMR) of 142 kt (73.1 m s^{-1}) in the southwestern quadrant and 163 kt (83.9 m s^{-1}) in the northeastern quadrant, 3) a surface wind speed estimate of 139 kt (71.5 m s^{-1}) based on the lowest 150-m layer average from a dropwindsonde, and 4) a surface pressure measurement of 936 hPa from a dropwindsonde with a surface wind speed of 12.3 m s^{-1}. The 163-kt observation was discounted at the time due to possible contamination from graupel.

The NHC discussion stated that the mission had been aborted due to extreme turbulence and graupel. The aircraft, flying at a prescribed pressure altitude of 700 hPa, in fact encountered flight-level horizontal wind gusts of over 83 m s^{-1}, and vertical wind speeds varying from 10 m s^{-1} downward to 31 m s^{-1} upward and back to about 7 m s^{-1} downward within 1 min. This led the plane to rise nearly 300 m and then return to its original pressure level within that time, almost all due to the vertical air motions encountered. The aforementioned

[a] Current affiliation: Department of Meteorology and Atmospheric Science, The Pennsylvania State University, University Park, Pennsylvania.

Corresponding author e-mail: Sim D. Aberson, sim.aberson@noaa.gov

DOI: 10.1175/MWR-D-16-0364.1

TABLE 1. Flight times and best track maximum sustained wind speeds and pressures during flights into Hurricane Felix.

Flight ID	Flight nominal time	Best track intensity (kt/m s^{-1})	Best track pressure (hPa)
070901h (NOAA42)	0000 UTC 2 Sep	65/33.4	993
070902i (NOAA43)	1200 UTC 2 Sep	90/46.3	981
070902h (NOAA42)	0000 UTC 3 Sep	145/74.6	930

eyewall dropwindsonde was serendipitously released during this 1-min period, providing some information on the thermodynamic structure of the feature that caused the event. These data, along with airborne Doppler radar data, provide a new dataset in features similar to those described in category 5 Hurricanes Hugo in 1989 (Marks et al. 2008), Isabel in 2003 (Aberson et al. 2006b), and Patricia in 2015 (Rogers et al. 2017). The following describes the data obtained in and around this feature. Section 2 is a description of the flight into Hurricane Felix and the event that led to the flight being aborted. The structure of Felix at the time using all available aircraft instrumentation is described in section 3, and conclusions are presented in section 4.

2. The flight into Hurricane Felix

NOAA conducted a series of flights into Hurricane Felix to gather Doppler wind data during an entire

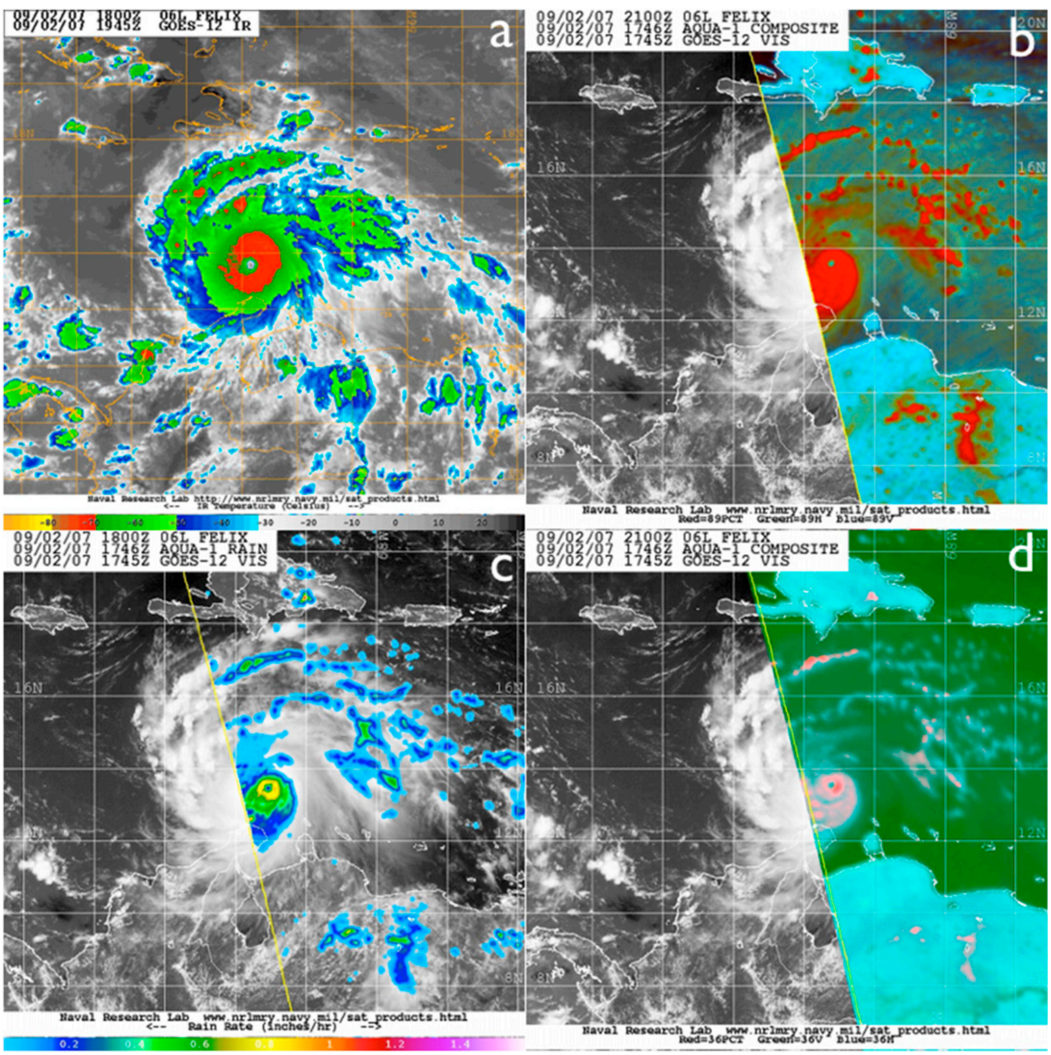

FIG. 1. Satellite imagery nearest the time of the eyewall penetration on 2 Sep 2007: (a) Geostationary Operational Environmental Satellite system infrared imagery at 1945 UTC (4-km resolution); the infrared channel allows for sensing of cloud type and height (temperature). (b) *Aqua* 85.5-GHz color composite at 1746 UTC (~15-km resolution); this shows ice scattering and provides a measure of precipitation. (c) *Aqua* retrieved surface rain at 1746 UTC (~15-km resolution). (d) *Aqua* 37-GHz color product at 1746 UTC (~15-km resolution); this channel shows low-level clouds and rain.

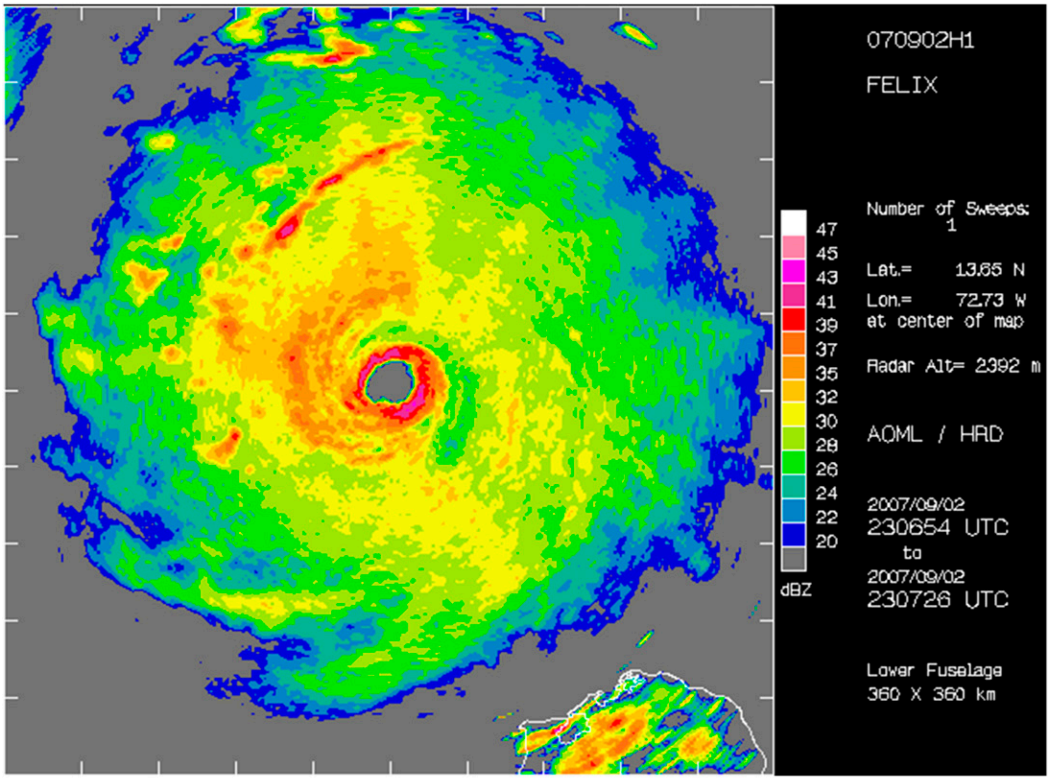

FIG. 2. Lower-fuselage radar reflectivity image from NOAA42 around 2307 UTC 2 Sep 2007. The aircraft (radar) is located at the center of the image.

tropical cyclone life cycle. The plan for the third flight was to depart St. Croix at 2000 UTC 2 September and approach Felix from the northeast, fly 105 n mi (1 n mi = 1.852 km) legs, each rotated 45° downwind from the endpoint of the previous leg, and then return to base. Felix was centered a little more than 100 km north of the Guajira Peninsula of Colombia (Fig. 1). NHC analyzed that Felix was moving toward the west-northwest (285°) at about 8 $m s^{-1}$ while rapidly intensifying into a major hurricane with a maximum sustained wind speed of about 110 kt (56.6 $m s^{-1}$) and minimum central sea level pressure of 964 hPa. Infrared satellite imagery showed that Felix had cloud-top temperatures <−70°C encircling a well-defined eye. A recent *Aqua* satellite pass with the Advanced Microwave Scanning Radiometer for Earth Observing System (AMSR-E; Ashcroft and Wentz 2000) showed a vertically aligned eyewall consisting of a heavy precipitation ring. Observers on an Air Force reconnaissance flight then in Felix observed a closed eyewall with a 12 n mi radius and a stadium effect; they found Felix to be small, with hurricane-force winds extending out only 15 n mi from the center in all quadrants, and gale-force winds extending only 40 n mi to the southwest and 90 n mi to the northeast. Felix was under very light (<3 $m s^{-1}$) deep-layer shear, over 28.5°C water, and the atmosphere was moist, all providing prime conditions for continued rapid intensification as it moved west-northwestward at about 15 kt (7.7 $m s^{-1}$).

NOAA42 approached the eye of Hurricane Felix around 2245 UTC 2 September. A single-sweep from the lower-fuselage radar (Jorgensen 1984; Fig. 2) showed a circular high-reflectivity region surrounding the eye. A few small rainbands were seen on the western side of the storm, with one strong outer band extending from north to west of the center. This structure was reminiscent of that of Hurricane Hugo when it was near maximum intensity (Marks et al. 2008, see their Fig. 2).

The flight-level horizontal wind speed[1] on the inbound leg (Fig. 3) increased to about 60 $m s^{-1}$ by 2251:30 UTC, then jumped to over 80 $m s^{-1}$ before a quick 25 $m s^{-1}$ decrease. The rapid wind speed changes occurred during a 10°–15° wind-direction shift. These changes correspond to horizontal wind shear values of about 8 and 40 $m s^{-1} km^{-1}$ outside and inside the maximum, respectively, using an aircraft ground speed of approximately 130 $m s^{-1}$. The SFMR-measured surface

[1] All wind measurements are presented in Earth-relative coordinates.

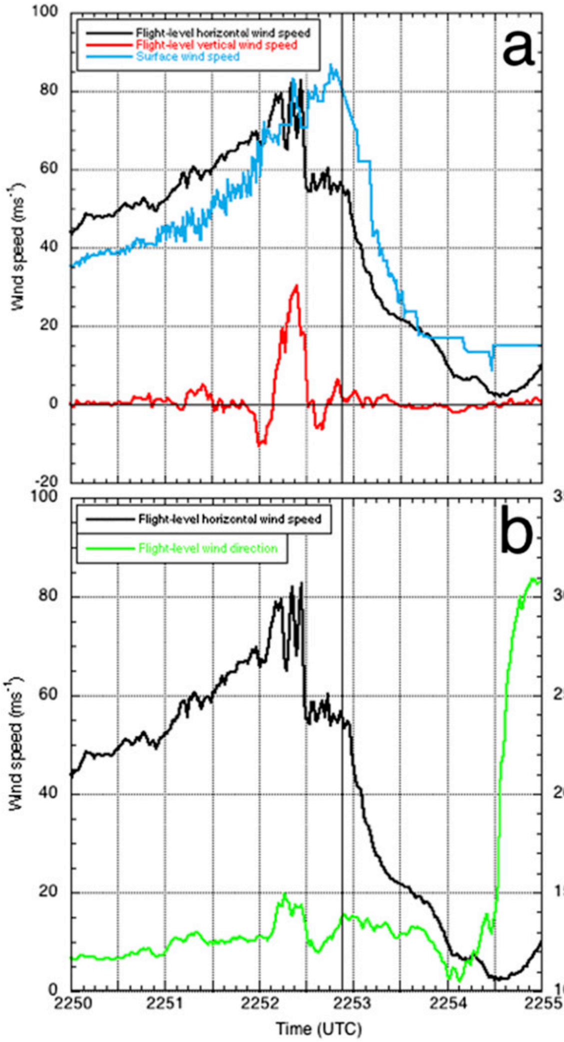

FIG. 3. Flight-level and surface wind data during the inbound leg into Hurricane Felix: (a) flight-level horizontal wind speed, vertical wind velocity, and surface wind speed; and (b) flight-level horizontal wind speed and direction. The black vertical line corresponds to the time of the release of a dropwindsonde.

FIG. 4. Aircraft radar altitude during the inbound leg into Hurricane Felix. The general decline in radar altitude from outside to inside the eye is due to the aircraft flying at a constant pressure altitude of 700 hPa.

wind speed continued to increase along the flight track reaching 86.7 m s^{-1} at a location 4 km inside the flight-level wind speed maximum. Concurrent with the flight-level wind speed maximum, the aircraft encountered a downdraft larger than 10 m s^{-1}, followed 20 s later by a nearly 31 m s^{-1} updraft, and 20 s later by another downdraft of almost 7 m s^{-1}; this corresponds to shear of the vertical wind of 18 m s^{-1} km^{-1}. The updraft marks the largest updraft a NOAA P3 has encountered during hurricane missions. The aircraft descended 200 m in about 40 s, before a quick rise and fall of more than 250 m in 20 s each (Fig. 4) during the vertical velocity fluctuations. The mission was aborted since these values are beyond aircraft specifications. The plane circled five times clockwise within the eye until finding a safe way to leave to the southwest (Fig. 5).

The plan was to release a dropwindsonde just inside the flight-level radius of maximum wind speed (RMW), near the surface RMW; the launch within 4 km of the extreme vertical and horizontal wind speed maxima in the northeastern eyewall was serendipitous (vertical line on Fig. 3). The temperature at the launch location was about 19.5°C with 60% relative humidity, suggesting that the instrument was released within the warm, dry hurricane eye (Fig. 6). The temperature cooled more than 2°C, and the humidity increased to near saturation during the first 1 km of descent. This suggests that the instrument fell into the relatively cool and moist eyewall, though the horizontal wind speed did not change. The instrument sensed increasing temperature during the remainder of the descent until reaching the low-level wind speed maximum where another temperature inversion was encountered.

The instrument entered a nearly −25 m s^{-1} downdraft below where the air first became saturated. The horizontal wind speed jumped to just over 100 m s^{-1} at 119 m before decreasing to only 18 m s^{-1} near the surface, for a vertical wind shear of more than 700 m s^{-1} km^{-1}; these shear values are eight orders of magnitude larger than those known to lead to the horizontal shearing instabilities and misocyclone development (Lee and Wilhelmson 1997). Below the base of the strong downdraft, the instrument was transported outward from the

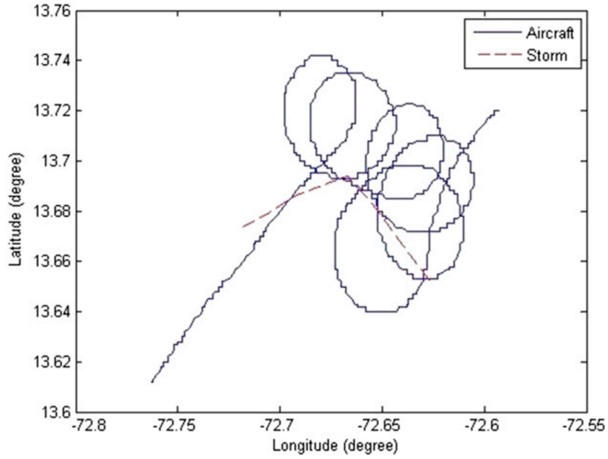

FIG. 5. Flight track and track of the flight-level center of Felix during the time NOAA42 was in the core of Hurricane Felix. NOAA42 entered Felix from the northeast at 2253:39 UTC and exited toward the southwest at 2307:48 UTC.

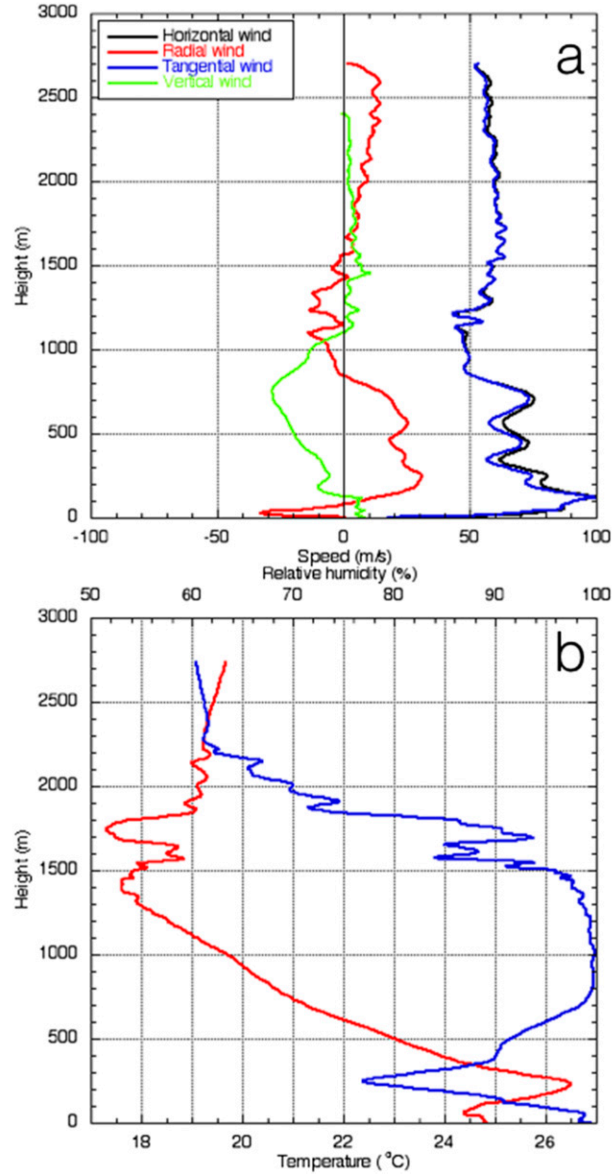

FIG. 6. Data from the dropwindsonde released at 2252 UTC 2 Sep 2007 in Hurricane Felix: (a) horizontal wind speed, and radial, tangential, and vertical wind velocities; and (b) temperature (red) and relative humidity (blue).

center of Felix, then inward near the surface, with the radial wind component reaching nearly 35 m s^{-1} in both directions, suggesting a meso- or misocyclone. This contrasts with the dropwindsonde released in the eyewall of Hurricane Isabel, which was also a category 5 hurricane (Aberson et al. 2006b). The temperature of the Isabel observation was cooler than that in Felix except within the boundary layer. In the Isabel observation, the temperature decreased less than 1°C below the aircraft, the relative humidity was always close to saturation, and the horizontal wind speed increased with decreasing altitude. That observation had large temperature deviations where the very strong updraft occurred, and the wind velocity variations were almost solely in the azimuthal direction. The Isabel dropwindsonde likely fell into an eyewall misovortex with very large vertical motions, whereas the Felix dropwindsonde began transmitting data within or just below the feature encountered at flight level before encountering another feature near the surface.

Very strong horizontal wind is hypothesized to occur when high-entropy air from the eye mixes into the eyewall (Persing and Montgomery 2003). This high-entropy air acts as an additional heat source to the eyewall, providing local convective instability (Eastin et al. 2005a,b; Braun 2002; Smith et al. 2005). This instability may spur local, strong convective updrafts and a subsequent horizontal-wind acceleration by concentrating the high angular momentum of the swirling flow, similar to that described in Persing and Montgomery (2003), but on a smaller scale. In Felix, the aircraft found the flight-level (now approximately 3000 m) wind center and released a dropwindsonde, and a third dropwindsonde was released in the southwest eyewall as the aircraft departed the eye. The wind speed and equivalent potential temperature (θ_e) profiles from the two eyewall soundings (Fig. 7) are similar down to about 1250-m altitude. Below this, where strong inward and outward radial motions exist, θ_e is up to 10 K higher in the northern eyewall than in the southern portion and is very close to that in the eye to about 350 m, further suggesting mixing between the eye and eyewall air due to strong radial winds. The wind speed in the northern eyewall is up to 40 m s^{-1} lower

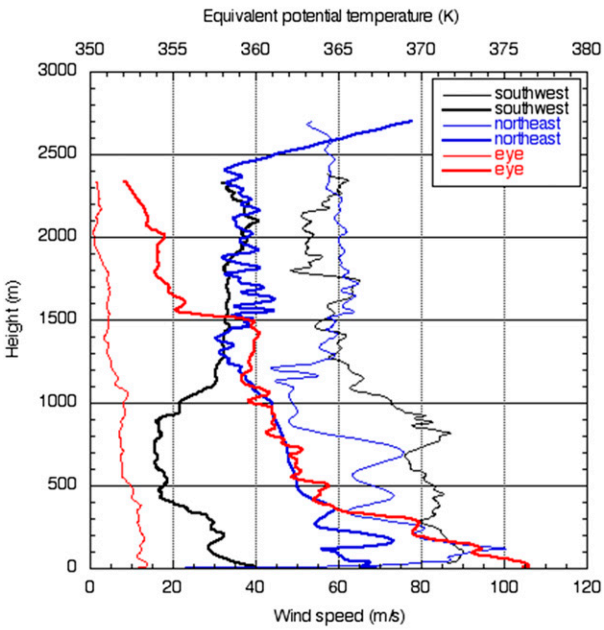

FIG. 7. Equivalent potential temperature (thick) and horizontal wind speed measurements (thin) from the three dropwindsondes released in the eye and eyewall of Hurricane Felix.

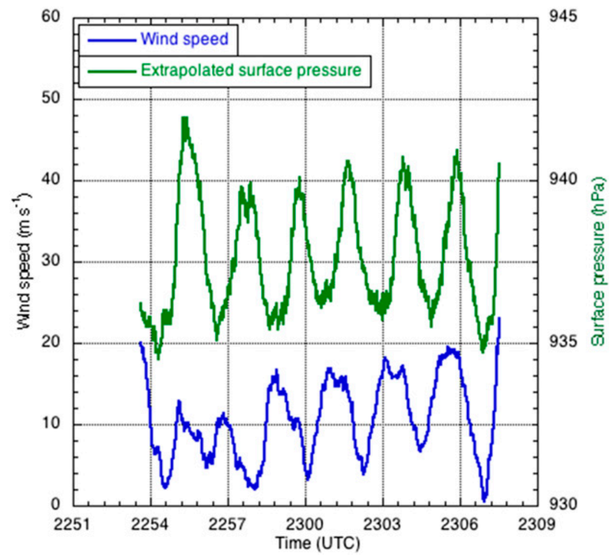

FIG. 8. Extrapolated surface pressure and flight-level wind speed during the time NOAA42 was in the eye of Hurricane Felix.

than that in the southern portion, except in the lowest 250 m of the profile. Using the eye and eyewall dropwindsonde data, the eye excess energy (Barnes and Fuentes 2010), a function of the difference in θ_e between the eye and the eyewall updrafts integrated through the layer where θ_e in the eye is higher than that in the eyewall, is calculated. The excess eye energy is $3.1 \times 10^6\,\mathrm{J\,m^{-2}}$ and $12.7 \times 10^6\,\mathrm{J\,m^{-2}}$ using the southwest and northeast measurements, respectively. The excess eye energy is likely underestimated in the northeast eyewall because that dropwindsonde moved into the eye in the boundary layer. The excess eye energy calculated from the northeast eyewall dropwindsonde data is comparable to that estimated by Barnes and Fuentes (2010) in Hurricane Lili (2002) during its rapid intensification phase.

The high-entropy air in the Felix eye had mixed into the eyewall by the observation time, and the local convective instability allowed for the rapid upward motion the aircraft encountered. The highest horizontal wind speed reported by the dropwindsonde released in the northeastern eyewall ($\sim$100 m s^{-1}) occurs at the θ_e maximum in the profile, adding further evidence that acceleration due to eye–eyewall mixing had occurred. In both eyewall soundings, the highest wind speeds are located in the lowest 150 m. Aberson et al. (2006b) speculate that these low-level features can reach the surface in convective downdrafts, leading to extreme localized damage as seen in Hurricane Andrew at landfall.

3. Storm structure

Marks et al. 2008 investigated a similar encounter during a flight into Hurricane Hugo on 15 September 1989. Both Hugo and Felix were at category 5 intensity and nearing the end of rapid intensification. Both hurricanes had a high-reflectivity ring surrounding a small eye, and a relative lack of rainbands outside (cf. Fig. 2 here with their Fig. 2). One important difference between the two encounters is in the flight altitudes (about 500 m in Hugo vs 3000 m in Felix). The radius of the maximum reflectivity in Hurricane Felix was about 11 km compared to about 12.5 km in Hugo; due to the outward slope of the eyewall with altitude, the eye of Felix was likely smaller than that of Hugo. The flight-level horizontal and vertical wind speeds were both higher in Felix than in Hugo. In both cases, the aircraft circled multiple times in the eye, providing unusual datasets for analysis, but, in the present case, three-dimensional kinematic analysis is not possible due to the failure of the aircraft Tail Doppler Radar except in the northeastern eyewall.

Figure 8 shows the estimated surface pressure and flight-level wind speed during the time NOAA42 circled within the eye of Felix. Surface-pressure and wind speed oscillations with a $\sim$1.5-min period and amplitudes of about 5 hPa and 10–12 m s^{-1}, respectively, are seen. Since the two oscillations are out of phase, the flight-level wind and surface-pressure centers were not collocated. The approximate locations of the two centers defined as the locations of the minima along the flight track are shown in Fig. 9a, and Fig. 9b shows the tracks

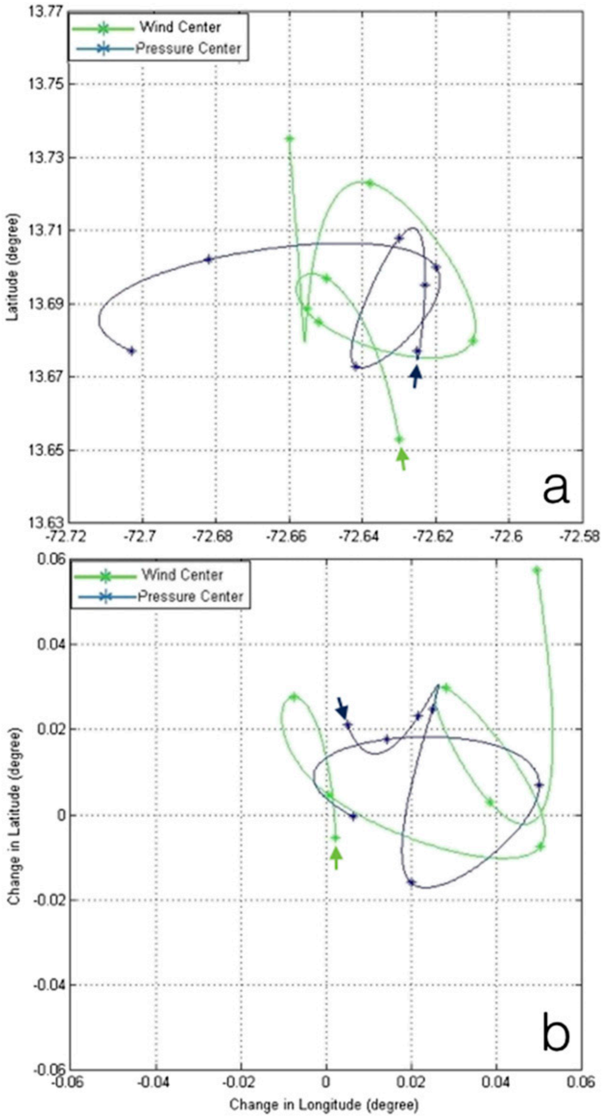

FIG. 9. Track of the flight-level wind and extrapolated surface pressure centers of Hurricane Felix in (a) Earth-relative coordinates, and (b) storm-relative coordinates. Arrows point to the starting locations and directions of motion.

relative to a smoothed track of the larger-scale flight-level wind centers (Willoughby and Chelmow 1982). A counterclockwise motion of the two centers with a 3-min period and radius of 3–5 km is evident, and both values are smaller than those seen in Hurricane Hugo; the translation speeds of the two centers was between 105 and 175 $m s^{-1}$, or quite a bit faster than the flow in the eyewall.

The flight-level data are decomposed into the primary vortex, represented by the values passed through a 100-s filter, and the perturbation (residual). The primary-vortex flight-level tangential wind speed is about the same on both the inbound and outbound legs (Fig. 10), whereas the primary-vortex surface wind speed from the SFMR is 82 and 70 $m s^{-1}$ on the inbound and outbound legs, respectively. Using the same technique as in Nolan et al. (2001) and Marks et al. (2008), the theoretical period of a trochoidal model in three-dimensional baroclinic vortices is just less than 28 min in this case. Unlike in Marks et al. (2008), this value is far larger than the measured 3-min period of the wind and pressure centers (Fig. 9b).

A Doppler radar data analysis is available only in the northeastern quadrant of Felix due to the radar system failure. The analysis shows two small areas of winds stronger than 80 $m s^{-1}$ at 0.5-km altitude where the dropwindsondes also sampled such winds (Fig. 11). The analyzed winds weakened with altitude up to 1.5 km, similar to what is shown in the dropwindsonde data, and then remained steady until about 7.5-km altitude when they again began to decrease. The wind speed maximum rotated from the east and northeast eyewall at low levels to the northern eyewall at 2.5-km altitude where it remained with increasing altitude. Because of the analysis resolution (1.5 km), no mesovortex signatures are seen in the wind direction, though the double wind speed maximum at low levels suggests two vorticity maxima there. A special analysis at 0.75-km resolution (not shown) is not appreciably different. The Earth-relative profile analysis (Fig. 12) shows an extended area of low-level outflow, further suggesting eye–eyewall mixing in this region. The profile also shows a strong increase in wind speed from flight-level (~3 km) to a maximum just above the surface (~150 m), verifying that the surface wind speed may indeed have been higher than that at flight level.

4. Discussion and conclusions

On 2 September 2007, NOAA42 encountered an intense downdraft–updraft–downdraft feature along with very strong horizontal winds in the northeastern eyewall of Hurricane Felix. This feature was similar to that penetrated during a flight in Hurricane Hugo about 18 years earlier, with the notable difference being the flight levels of the two encounters. Both Hurricanes Felix and Hugo were small, yet very intense tropical cyclones nearing the end of a rapid intensification episode. The radar signature of each was mainly made up of a ring of high reflectivity surrounding a small eye with only minimal rainbands in evidence. The pressure deviations in the features encountered were about the same in the two hurricanes (on the order of 10 hPa).

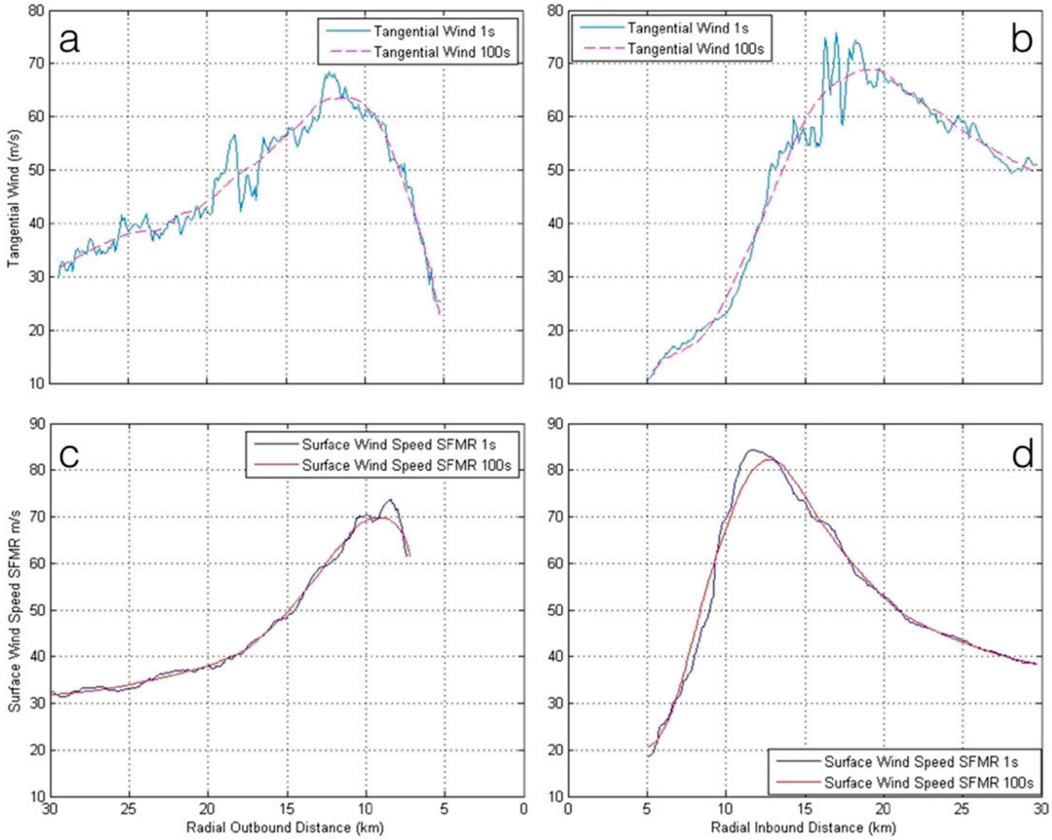

FIG. 10. Measured and smoothed flight-level tangential and surface wind speed on the (a),(c) outbound and (b),(d) inbound legs from the penetration of Hurricane Felix. Figures are shown from west to east, so time increases toward the left.

Despite these similarities, large differences also exist. The horizontal wind speed perturbations in the feature encountered in Felix were about half the size of that in Hugo. The theoretical period of a trochoidal model in three-dimensional baroclinic vortices is far larger than what was seen in the flight-level data in Felix, unlike in Hugo where the theoretical and measured values corresponded well. The reason for the discrepancy is unknown, but it is noted that the theoretical period is longer than the aircraft sampling time within the eye. It is possible that multiple centers were encountered in Felix unlike the single one in Hugo, though the data suggest that a wavenumber-2 pattern like that seen in Hurricane Erin (Aberson et al. 2006a) is unlikely; the limited data in time preclude identification of higher wavenumber features than this. The rapid translation of the feature around the eyewall suggests the possibility that it could be associated with one or multiple misocyclones similar to that encountered in Hurricane Isabel (Aberson et al. 2006b).

The frequency of these features and their ultimate importance in the structural evolution remain research questions. Many very intense tropical cyclones have been sampled with aircraft without encountering these extreme events. It is unknown whether they have been missed by the relatively sparse observations available, because aircraft tend to deviate around the most intense eyewall convection, or if they are truly rare. Stern et al. (2016) found using dropwindsonde data that extreme updrafts (with upward vertical wind speeds greater than $10\,\mathrm{m\,s^{-1}}$) were commonly observed just inside the flight-level RMW in intense (categories 4 and 5) tropical cyclones during periods of small intensity change. Since these extreme events are even rarer in tropical cyclones before and during rapid intensification than in those maintaining high intensity, it may be that these processes are important for maintenance of extreme intensity rather than for extreme intensification rates themselves. In this case, though, Felix was at the end of its rapid intensification period, and the eye excess energy calculation suggests that high-θ_e air was mixed from the eye to the eyewall by this feature and possibly others. Questions also remain as to whether and how these features affect tropical cyclone structure, and whether

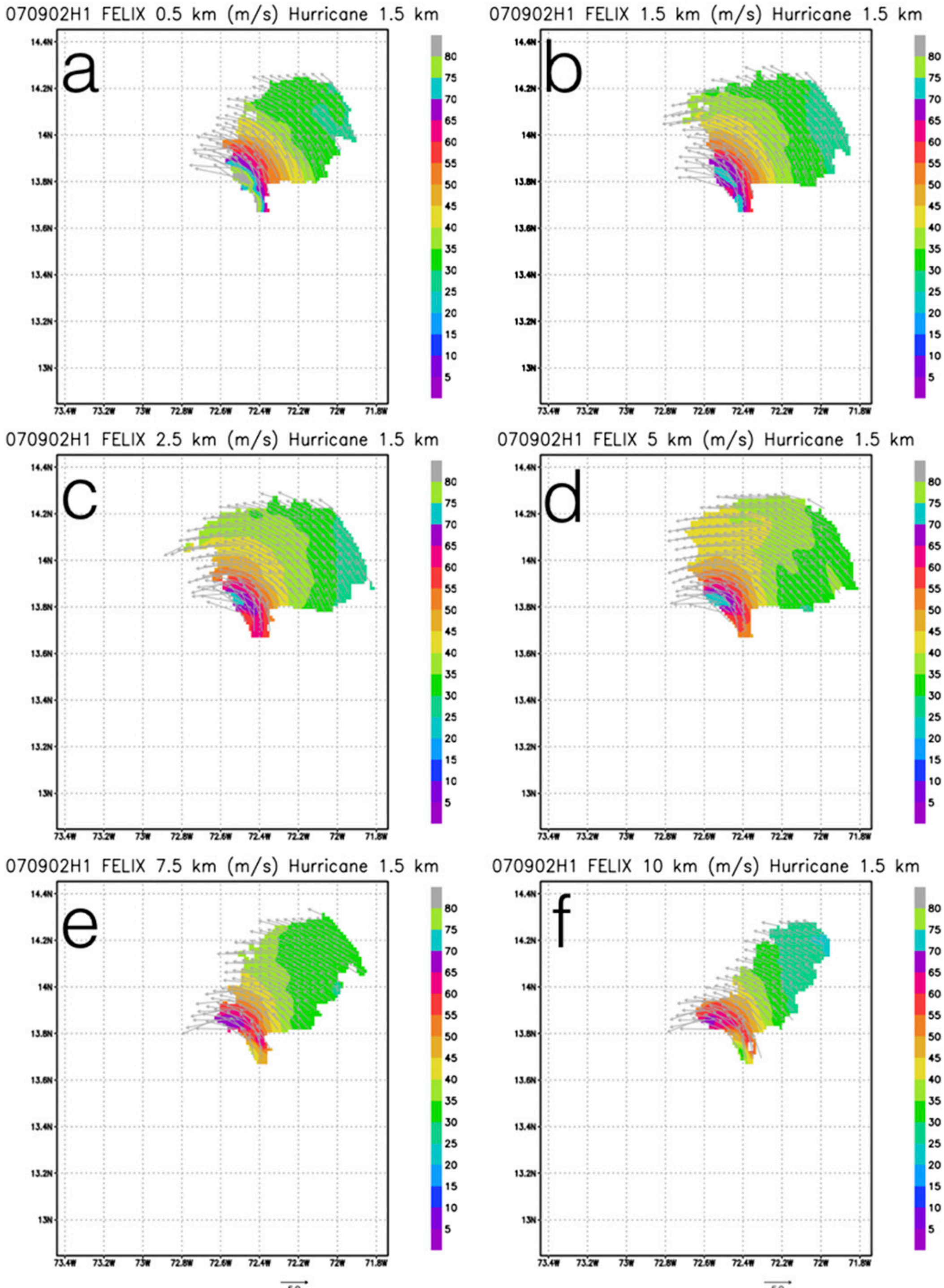

FIG. 11. Doppler radar wind analyses of Hurricane Felix at 1.5-km resolution at (a) 0.5-, (b) 1.5-, (c) 2.5-, (d) 5-, (e) 7.5-, and (f) 10-km altitudes.

they are translated downward impacting the surface, especially during landfall events. Recent very high-resolution simulations have been able to capture these features (Stern et al. 2016), but their importance for numerical forecasts remains unknown. It is clear, though, that improved understanding of these features would enhance the safety of flights into very intense tropical cyclones.

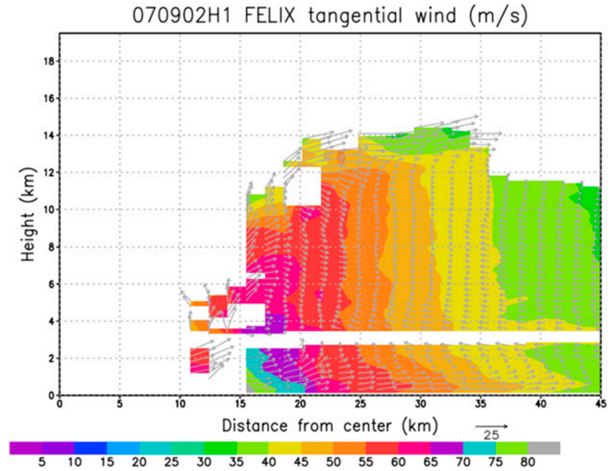

FIG. 12. Wind-velocity profile analysis along the flight track from the inbound leg in Hurricane Felix. Tangential wind speed is shaded, and arrows represent the radial and vertical wind velocity.

Acknowledgments. The authors wish to thank the flight crew of NOAA42, especially pilots Carl Newman and Tom Strong, flight director Tom Shepard, flight engineer Steve Wade, and navigator Tim Gallagher, for safely returning the aircraft and the scientific crew to base. The third author was supported during the work by the NOAA Education Partnership Program. The radar wind analyses were made by John Gamache; the large-scale track of Felix was created by Neal Dorst. Garpee Barleszi, Mike Jankulak, Frank Marks, Rob Rogers, and an anonymous reviewer provided very helpful comments to the original version of the manuscript.

REFERENCES

Aberson, S. D., J. P. Dunion, and F. D. Marks, 2006a: A photograph of a wavenumber-2 asymmetry in the eye of Hurricane Erin. *J. Atmos. Sci.*, **63**, 387–391, doi:10.1175/JAS3593.1.

——, M. Black, M. T. Montgomery, and M. Bell, 2006b: Hurricane Isabel (2003): New insights into the physics of intense storms. Part II: Extreme localized wind. *Bull. Amer. Meteor. Soc.*, **87**, 1349–1354, doi:10.1175/BAMS-87-10-1349.

Ashcroft, P., and F. J. Wentz, 2000: AMSR algorithm theoretical basis document. RSS Tech. Rep. 121599B-1, 27 pp.

Barnes, G. M., and P. Fuentes, 2010: Eye excess energy and the rapid intensification of Hurricane Lili (2002). *Mon. Wea. Rev.*, **138**, 1446–1458, doi:10.1175/2009MWR3145.1.

Braun, S. A., 2002: A cloud-resolving simulation of Hurricane Bob (1991): Storm structure and eyewall buoyancy. *Mon. Wea. Rev.*, **130**, 1573–1592, doi:10.1175/1520-0493(2002)130<1573:ACRSOH>2.0.CO;2.

Brennan, M. J., R. D. Knabb, M. Mainelli, and T. B. Kimberlain, 2009: Atlantic hurricane season of 2007. *Mon. Wea. Rev.*, **137**, 4061–4088, doi:10.1175/2009MWR2995.1.

Eastin, M. D., W. M. Gray, and P. G. Black, 2005a: Buoyancy of convective vertical motions in the inner core of intense hurricanes. Part I: General statistics. *Mon. Wea. Rev.*, **133**, 188–208, doi:10.1175/MWR-2848.1.

——, ——, and ——, 2005b: Buoyancy of convective vertical motions in the inner core of intense hurricanes. Part II: Case studies. *Mon. Wea. Rev.*, **133**, 209–227, doi:10.1175/MWR-2849.1.

Jorgensen, D. F., 1984: Mesoscale and convective-scale characteristics of mature hurricanes. Part I: General observations by research aircraft. *J. Atmos. Sci.*, **41**, 1268–1286, doi:10.1175/1520-0469(1984)041<1268:MACSCO>2.0.CO;2.

Lee, B. D., and R. B. Wilhelmson, 1997: The numerical simulation of nonsupercell tornadogenesis. Part I: Initiation and evolution of pretornadic misocyclone circulations along a dry outflow boundary. *J. Atmos. Sci.*, **54**, 32–60, doi:10.1175/1520-0469(1997)054<0032:TNSONS>2.0.CO;2.

Marks, F. D., P. G. Black, M. T. Montgomery, and R. W. Burpee, 2008: Structure of the eye and eyewall of Hurricane Hugo (1989). *Mon. Wea. Rev.*, **136**, 1237–1259, doi:10.1175/2007MWR2073.1.

Nolan, D. S., M. T. Montgomery, and L. D. Grasso, 2001: The wavenumber-one instability and trochoidal motion of hurricane-like vortices. *J. Atmos. Sci.*, **58**, 3243–3270, doi:10.1175/1520-0469(2001)058<3243:TWOIAT>2.0.CO;2.

Persing, J., and M. T. Montgomery, 2003: Hurricane superintensity. *J. Atmos. Sci.*, **60**, 2349–2371, doi:10.1175/1520-0469(2003)060<2349:HS>2.0.CO;2.

Rogers, R. F., and Coauthors, 2017: Rewriting the tropical record books: The extraordinary intensification of Hurricane Patricia (2015). *Bull. Amer. Meteor. Soc.*, doi:10.1175/BAMS-D-16-0039.1, in press.

Smith, R. K., M. T. Montgomery, and H. Zhu, 2005: Buoyancy in tropical cyclones and other rapidly rotating atmospheric vortices. *Dyn. Atmos. Oceans*, **40**, 189–208, doi:10.1016/j.dynatmoce.2005.03.003.

Stern, D. P., G. H. Bryan, and S. D. Aberson, 2016: Extreme updrafts and wind speeds measured by dropsondes in tropical cyclones. *Mon. Wea. Rev.*, **144**, 2177–2204, doi:10.1175/MWR-D-15-0313.1.

Willoughby, H. E., and M. B. Chelmow, 1982: Objective determination of hurricane tracks from aircraft observations. *Mon. Wea. Rev.*, **110**, 1298–1305, doi:10.1175/1520-0493(1982)110<1298:ODOHTF>2.0.CO;2.